144, 841 (1965).
[13]V. L. Trimble and K. S. Thorne, Astrophys. J. 156, 1013 (1969).
[14]N. M. Shakhovskoi, Astron. Zh. 41, 1042 (1964) [Sov. Astron. – AJ 8, 833 (1965)].
[15]K. H. Prendergast and G. R. Burbidge, Astrophys. J. Letters 151, L83 (1968).
[16]Ya. B. Zel'dovich and I. D. Novikov, *Stars and Relativity* (University of Chicago Press, Chicago, 1971).

PHYSICAL REVIEW D VOLUME 7, NUMBER 10 15 MAY 1973

Maximally Slicing a Black Hole*

Frank Estabrook and Hugo Wahlquist
Jet Propulsion Laboratory, California Institute of Technology, Pasadena, California 91103

Steven Christensen, Bryce DeWitt, Larry Smarr, and Elaine Tsiang
Relativity Center, Department of Physics, The University of Texas, Austin, Texas 78712
(Received 20 November 1972)

Analytic and computer-derived solutions are presented of the problem of slicing the Schwarzschild geometry into asymptotically-flat, asymptotically-static, maximal spacelike hypersurfaces. The sequence of hypersurfaces advances forward in time in both halves ($u \geq 0$, $u \leq 0$) of the Kruskal diagram, tending asymptotically to the hypersurface $r = \frac{3}{2}M$ and avoiding the singularity at $r = 0$. Maximality is therefore a potentially useful condition to impose in obtaining computer solutions of Einstein's equations.

We report (1) the results of a computer study of the problem of maximally slicing the Schwarzschild geometry and (2) an analytic solution of the same problem. The computer study was part of a much larger program currently under way at Texas to study the behavior of colliding black holes. Data obtained in such studies will be of interest to two groups of physicists: those who wish to learn something about the gravitational energy radiated to infinity and those who are curious about details of the growth and coalescence of event horizons and the dynamical processes taking place near the singularities hidden inside. In order to obtain data of use to both groups one must employ coordinate systems that guarantee the following:
(A) The metric must pass smoothly to a familiar metric (e.g., spherical Minkowskian) at infinity.
(B) The hypersurfaces $x^0 =$ constant must be spacelike and must penetrate the event horizon(s).
(C) The metric must remain nonsingular for the duration of the computation.

It has long been speculated that a good way of securing these conditions is to require the hypersurfaces $x^0 =$ constant to be maximal.[1] The maximality condition is expressed by the statement

$$\gamma^{ij}K_{ij} = 0, \tag{1}$$

where, for each x^0, γ^{ij} and K_{ij} are, respectively, the (contravariant) 3-metric and second fundamental form on the corresponding hypersurface. When (1) holds, Einstein's vacuum equations reduce to

$$K_{ij}K^{ij} = {}^{(3)}R \equiv \gamma^{ij}\,{}^{(3)}R_{ij}, \tag{2}$$

$$K^{ij}{}_{,j} = 0, \tag{3}$$

$$K_{ij,0} = \alpha\,{}^{(3)}R_{ij} - \alpha_{,ij} - 2\alpha K_{ik}K^{k}{}_{j} + \pounds_{\beta}K_{ij}, \tag{4}$$

where, for each x^0, ${}^{(3)}R_{ij}$ is the curvature tensor of the corresponding hypersurface, α and β_i are, respectively, the lapse function and shift vectors relating this hypersurface to its neighbors, dots denote covariant differentiation in the hypersurface, and indices are raised and lowered by means of the 3-metric.[2]

Equation (1) may be treated on a par with the so-called initial-data constraints (2) and (3). If these three equations are imposed on an initial hypersurface then they will automatically be maintained on each succeeding hypersurface by the dynamical equation (4) together with the following condition on the lapse function[3]:

$$\alpha_{,i}{}^{i} = {}^{(3)}R\alpha. \tag{5}$$

In an effort to determine whether the maximality condition in fact secures conditions (A), (B), (C) above, and whether solution of Eqs. (1)–(5) is practical on the computer, four of us (S.C., B.D., L.S., E.T.) undertook to run a test on the simplest nontrivial example: the Schwarzschild black hole.

Constraints (1), (2), and (3) were satisfied by choosing the initial hypersurface to be the u axis in the familiar Kruskal plane.[4] Equations (4) and

(5) were then solved as difference equations subject to the boundary condition that the lapse function α become unity at spatial infinity and be constant over the initial hypersurface. The diffusion-relaxation technique was used on Eq. (5) while standard second-order methods with stability constraints on the time steps were used on Eq. (4). The mesh consisted of 25 points. The results are shown in Figs. 1 and 2.

Figure 1 depicts the progression of hypersurfaces $x^0 =$ constant in the Kruskal quadrant $u > 0$, $v > 0$. Each curve represents a maximal slice through the Schwarzschild space-time, with topology $S^2 \times R$. An accurate metric visualization of these slices can be obtained by suppressing an "ignorable" dimension (arising from the spherical symmetry) and embedding the result as a surface of revolution in a Euclidean 3-space. The curves that generate the surfaces of revolution are shown in Fig. 2. Strictly speaking, only half of each curve is shown. In the maximally extended Schwarzschild geometry each hypersurface consists of two congruent asymptotically flat sheets connected by an Einstein-Rosen bridge; only the upper sheet is shown in the figures.

The condition that the lapse function be constant on the initial hypersurface guarantees that the subsequent hypersurfaces generated by the computer will not be trivial static hypersurfaces $t =$ constant (in standard Schwarzschild coordinates) for which time runs forward on one sheet and backward on the other. Here time is forced to run forward on both sheets.

It is immediately apparent from Figs. 1 and 2 that the maximal hypersurfaces avoid the singularity at $r = 0$. Indeed, so well do they avoid the singularity that the inevitable contraction of the Einstein-Rosen bridge, associated with upward motion in the Kruskal plane, is arrested long before "pinch-off" occurs. Instead of pinching off, the bridge merely stretches. This behavior can be understood qualitatively as follows: The initial hypersurface has the metric of a 3-paraboloid. If it were a 2-paraboloid, it would have negative (scalar) curvature, but as a 3-surface it has *vanishing* ${}^{(3)}R$. As soon as the hypersurface moves off the u axis in the Kruskal plane, the bridge begins to stretch and its central portion begins to assume the shape of a 3-cylinder. A 3-cylinder, in contrast to a 3-paraboloid, has positive curvature (essentially that of its generating 2-spheres). When ${}^{(3)}R$ becomes positive, Eq. (5) forces the lapse function to become concave upward (as a function of r) at the center of the bridge. Because α is held equal to unity at infinity, it quickly plummets toward zero in the cylindrical region and causes the bridge to stabilize at a constant r.

The numbers generated by the computer show the stabilization radius to be very nearly equal to $1.5M$, where M is the mass of the black hole.[5] The question immediately arises: Is the coefficient exactly $\frac{3}{2}$? An affirmative answer is strongly suggested by the fact that the hypersurface $r = 1.5M$ is itself maximal, as one may readily

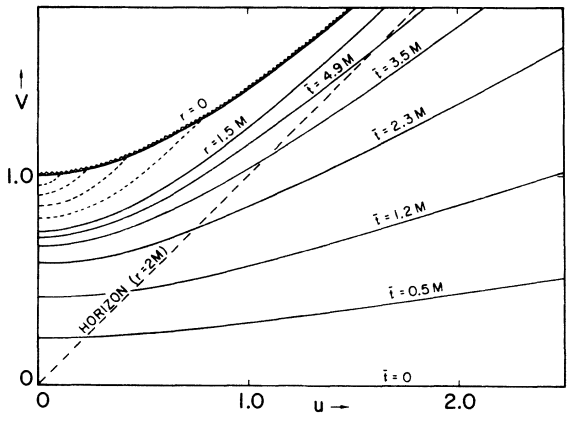

FIG. 1. The solid curves are the projections of the hypersurfaces $x^0 (= \bar{t}) =$ constant in the Kruskal plane. Each tends asymptotically to a straight line $t =$ constant. As $x^0 (= \bar{t}) \to \infty$ the projections converge to the curve $r = 1.5M$. The dotted curves are the projections of another family of maximal hypersurfaces, lying inside $r = 1.5M$ (see Ref. 8).

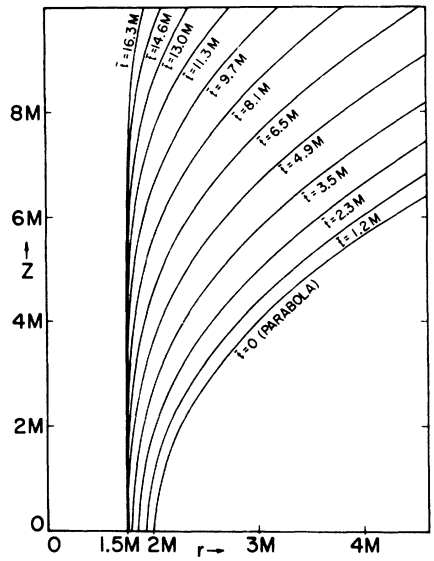

FIG. 2. Generating curves for the maximal 3-geometries. Choose a value of $\bar{t}$. Rotate the corresponding curve about the z axis. The result is a 2-surface having the metric properties of a symmetric (e.g., equatorial) slice through the maximal hypersurface corresponding to that value of $\bar{t}$.

check.

While the computer analysis was being carried out, two of us (F.E. and H.W.) were obtaining an explicit analytic solution of the problem. The solution was first discovered with the aid of a previously developed spacelike dyadic formalism[6,7] (analogous to the Newman-Penrose null-tetrad formalism employed in radiation studies), which is particularly well suited to problems of the present type. Here, however, the solution will be derived straight from the equations used by the computer to show that what the computer can do we can do better.

It proves convenient to start from a line element having the form

$$ds^2 = (-\alpha^2 + \gamma^{-1}\beta^2)d\bar{t}^2 + 2\beta d\bar{t}dr + \gamma dr^2 + r^2(d\theta^2 + \sin^2\theta\, d\varphi^2), \tag{6}$$

where α, β, and γ are functions of r and $\bar{t}$ only. Evidently r, θ, and φ are standard Schwarzschild coordinates, but $\bar{t}$ is not. In these coordinates Eq. (1) takes the form

$$-(\ln\gamma)_{,\bar{t}} + \beta\gamma^{-1}[\ln(\beta^2\gamma^{-1}r^4)]_{,r} = 0. \tag{1'}$$

This equation may be used to eliminate $\bar{t}$ derivatives of γ from Eqs. (2), (3), and (4), which then simplify, respectively, to

$$3\alpha^{-2}\beta^2\gamma^{-1} = \gamma - 1 - r(\ln\gamma)_{,r}, \tag{2'}$$

$$[\ln(\alpha^{-1}\beta\gamma^{-1}r^2)]_{,r} = 0, \tag{3'}$$

$$[\ln(\alpha^{-1}\beta)]_{,\bar{t}} = (3\beta\gamma^{-1} + \alpha^2\beta^{-1}\gamma - \alpha^2\beta^{-1})r^{-1} + 3\gamma^{-1}\beta_{,r} + \tfrac{1}{2}(\alpha^2\beta^{-1} - 4\beta\gamma^{-1})(\ln\gamma)_{,r} - (\beta\gamma^{-1} + \alpha^2\beta^{-1})(\ln\alpha)_{,r}. \tag{4'}$$

Finally, Eq. (5) becomes

$$\alpha_{,rr} + 2r^{-1}\alpha_{,r} - \tfrac{1}{2}(\ln\gamma)_{,r}\alpha_{,r} = 2r^{-2}[\gamma - 1 - r(\ln\gamma)_{,r}]\alpha. \tag{5'}$$

Equation (3') immediately yields

$$\beta = \alpha\gamma T r^{-2}, \tag{7}$$

where T is a function of $\bar{t}$ only. Insertion of this result into Eq. (2') yields

$$\gamma^{-1}{}_{,r} = -(\gamma^{-1} - 1 + 3T^2r^{-4})r^{-1}, \tag{8}$$

a linear first-order equation with the solution

$$\gamma^{-1} = 1 - 2Mr^{-1} + T^2r^{-4}, \tag{9}$$

where the constant of integration M is a function of $\bar{t}$ only. If one now makes use of Eq. (7) to eliminate β from Eqs. (1') and (4'), and then invokes Eq. (9), one finds that Eq. (1') reduces to

$$(\alpha\gamma^{1/2})_{,r} = \gamma^{3/2}(T^{-1}M_{,\bar{t}}r - T_{,\bar{t}}r^{-2}), \tag{10}$$

while Eq. (4') tells us simply that M must be $\bar{t}$-independent. The complete analytic solution of the problem, which incorporates the condition that α become unity as $r \to \infty$, is therefore given by Eqs. (7) and (9) together with the particular integral of (10):

$$\alpha = (1 - 2Mr^{-1} + T^2r^{-4})^{1/2} \times\left[1 + \frac{T_{,\bar{t}}}{M}\int_0^{Mr^{-1}}(1 - 2x + T^2M^{-4}x^4)^{-3/2}dx\right]. \tag{11}$$

As a consistency check, one may verify by straightforward computation that Eq. (5'), which is a consequence of Eqs. (1') to (4'), is identically satisfied by (7), (9), and (11).

The $\bar{t}$ dependence of T remains thus far completely undetermined, because attention has been confined to a single sheet of the 3-geometry. The dependence may be fixed by imposing the requirement of smoothness across the Einstein-Rosen bridge. This is most easily done by passing to standard Schwarzschild coordinates $t(\bar{t}, r), r, \theta, \varphi$. It is readily verified that $t(\bar{t}, r)$ satisfies the differential equations

$$\partial t/\partial\bar{t} = \alpha\gamma^{1/2}, \tag{12}$$

$$\partial t/\partial r = \gamma^{1/2}(2Mr^{-1} - 1)^{-1}Tr^{-2}. \tag{13}$$

Equation (13) is solved by

$$t = TM^{-1}\int_{Mr^{-1}}^{X(T)}(2x - 1)^{-1}(1 - 2x + T^2M^{-4}x^4)^{-1/2}dx, \tag{14}$$

which also satisfies Eqs. (11) and (12) provided the function $X(T)$ is required to satisfy

$$dX/dT = T^{-1}(2X - 1)(1 - 2X + T^2M^{-4}X^4)^{1/2} \times\left[\frac{M}{T_{,\bar{t}}} + \int_0^X(1 - 2x + T^2M^{-4}x^4)^{-3/2}dx\right]. \tag{15}$$

In Schwarzschild coordinates the requirement of smoothness across the bridge (in the region $r < 2M$) is $t \to 0$, $\partial t/\partial r \to \infty$ as r approaches its smallest value $r_{\min}$ (at the center of the bridge). Applying this requirement to Eqs. (13) and (14) one sees that $r_{\min}$ must be $M/X(T)$, where $X(T)$ is the smaller of the two real roots[8] of the quartic $1 - 2x + T^2M^{-4}x^4$. By a careful limiting procedure one may verify that Eq. (15) is automatically satisfied when $X(T)$ is a root. Because t and $\bar{t}$ must coincide at spatial infinity (modulo a constant which may be set equal to zero), Eq. (14) now yields the desired relation between $\bar{t}$ and T:

$$\bar{t} = TM^{-1} \int_0^{X(T)} (2x-1)^{-1}(1-2x+T^2M^{-4}x^4)^{-1/2}dx\,. \tag{16}$$

Here the integration across the pole at $x = \frac{1}{2}$ is taken in the sense of the principal value.

For each value of T (or $\bar{t}$) Eq. (14) yields a space-time plot of the corresponding hypersurface. When converted into Kruskal coordinates, this plot takes precisely the form of one of the curves shown in Fig. 1, thus confirming the accuracy of the computer results. With care one may also derive the initial-value limits $T \to 0$, $dT/dt \to 1$, $\alpha \to 1$ as $\bar{t} \to 0$.

The integral (16) diverges when the two real roots of the quartic coincide. This occurs at $T = \frac{3}{4}\sqrt{3}\,M^2$, $X = \frac{2}{3}$. In this limit one finds $\bar{t} \to \infty$, $\alpha \to 0$, $r \to M/X = \frac{3}{2}M$, which implies that the hypersurface has become an infinitely long cylinder of radius $1.5M$. This confirms rigorously the stabilization effect discovered with the computer.

One may conclude from these results that the maximality condition is workable in computer solutions of Einstein's equations and that it very likely guarantees the conditions (A, B, C) mentioned at the beginning. There are, however, two considerations that may prevent one from adopting it in many cases: (1) Although the diffusion-relaxation method used to solve the elliptic lapse-function equation [Eq. (5)] was found to converge rapidly after the first few time steps ($\bar{t} > 2M$), the equation must be re-solved every time step, whatever method is used. This can present storage and real-time complications for large meshes. (2) Our actual program assumed a vanishing shift vector and a line element that differed somewhat from Eq. (16). In consequence, our coordinate mesh was gradually sucked down the black hole as the Einstein-Rosen bridge stretched. In order to avoid this phenomenon it is necessary to use an outward-pointing shift vector. What sort of equation should be introduced in non-spherically-symmetric situations to govern the growth of the shift vector is presently unknown.

Note added. After submitting this paper we learned that Bruce L. Reinhart has recently obtained identical mathematical results by introducing a simple orthonormal frame. We are indebted to Professor Reinhart for communicating his results to us.

---

*Work at The University of Texas supported in part by a grant from the National Science Foundation and, at the Jet Propulsion Laboratory, California Institute of Technology, under Contract No. NAS7-100, sponsored by the National Aeronautics and Space Administration.

[1]In a positive-definite manifold the analogous hypersurfaces are *minimal* and are similar to soap films or stretched rubber membranes.

[2]The 4-metric of space-time is

$$ds^2 = (-\alpha^2 + \beta_i\beta^i)(dx^0)^2 + 2\beta_i\,dx^i dx^0 + \gamma_{ij}\,dx^i dx^j$$

and K_{ij} is given by

$$K_{ij} = \tfrac{1}{2}\alpha^{-1}(-\gamma_{ij,0} + \mathcal{L}_\beta \gamma_{ij}),$$

$\mathcal{L}_\beta$ denoting the Lie derivative with respect to β_i.

[3]Cf. B. S. DeWitt, Phys. Rev. 160, 1113 (1967).

[4]M. D. Kruskal, Phys. Rev. 119, 1743 (1960).

[5]We use units in which $c = G = 1$.

[6]F. B. Estabrook and H. D. Wahlquist, J. Math. Phys. 5, 1629 (1964).

[7]H. D. Wahlquist and F. B. Estabrook, Phys. Rev. 156, 1359 (1967).

[8]A second family of smooth maximal hypersurfaces is obtained by taking

$$t = -TM^{-1}\int_{Y(T)}^{Mr^{-1}} (2x-1)^{-1}(1-2x+T^2M^{-4}x^4)^{-1/2}dx,$$

where $Y(T)$ is the larger real root of the quartic and the range of T is now

$$-\tfrac{3}{4}\sqrt{3}\,M^2 \le T \le 0.$$

All members of this family intersect the $r = 0$ singularity and grow outward to the limiting $r = \frac{3}{2}M$ surface, lying always completely inside the horizon. They are shown as dotted lines in Fig. 1. This family and the first family together completely fill the Kruskal diagram with spacelike maximal hypersurfaces. Members of the second family, however, cannot be conveniently visualized as surfaces of revolution in a Euclidean space.